

Vertex-corrected tunneling inversion in superconductors: Pb

J. K. Freericks^(a), E. J. Nicol^(b), A. Y. Liu^(a), and A. A. Quong^(c).

^(a) *Department of Physics, Georgetown University, Washington, DC 20057-0995*

^(b) *Department of Physics, University of Guelph, Guelph, ON N1G 2W1, Canada*

^(c) *Sandia National Laboratories, Livermore, CA 94551-0969*

(October 3, 2018)

Abstract

The McMillan-Rowell tunneling inversion program, which extracts the electron-phonon spectral function $\alpha^2F(\Omega)$ and the Coulomb pseudopotential μ^* from experimental tunneling data, is generalized to include the lowest-order vertex correction. We neglect the momentum dependence of the electron-phonon matrix elements, which is equivalent to using a local approximation. The perturbation theory is performed on the imaginary axis and then an exact analytic continuation is employed to produce the density of states on the real axis. Comparison is made with the experimental data for Pb.

Typeset using REVTeX

© 1996 by the authors. Reproduction of this article by any means is permitted for non-commercial purposes.

The theory of low-temperature superconductors is one of the most accurate theories in condensed-matter physics. Agreement to better than one part in 10^4 is common between the tunneling density of states (DOS) measured experimentally and that calculated with an extracted electron-phonon spectral function $\alpha^2F(\Omega)$ and Coulomb pseudopotential μ^* . The reason why the agreement is so good is due to Migdal's theorem [1], as formulated by Eliashberg [2] in the superconducting state, which says that there is a small parameter in the theory, namely the ratio of the phonon energy scale to the electronic energy scale, that guarantees the rapid convergence of the perturbative expansion. However in some recently discovered materials, that are believed to be electron-phonon superconductors, the ratio of the phonon to electronic energy scale is no longer as small. Two examples are $\text{Ba}_{1-x}\text{K}_x\text{BiO}_3$ [3] and the doped fullerenes [4] which have relatively high transition temperatures. This motivates the need for a theory that includes the effects of the so-called vertex corrections, which are neglected in the conventional Migdal-Eliashberg formalism. In this contribution, we present a generalization of the McMillan-Rowell [5] tunneling-inversion program to include the lowest-order effects of vertex corrections in the local approximation, and apply the new formalism to the low-temperature superconductor Pb to illustrate how vertex corrections can be incorporated into such an analysis, and to determine, quantitatively, the accuracy of the Migdal-Eliashberg formalism.

Recent work on incorporating vertex corrections into the theory of superconductivity [6–9] has illustrated some of their qualitative effects: If one adopts the conventional approximation of assuming a constant electronic DOS and neglecting the momentum dependence of the electron-phonon matrix elements, then the vertex corrections will suppress T_c and the isotope coefficient α . Incorporation of either momentum dependence to the matrix elements, or nonconstant DOS can lead to enhancements to T_c and α . Little is known about how large these effects can be in real materials, but they have been verified for model systems by comparing vertex-corrected theories [9] to the exact solution of electron-phonon models in the infinite-dimensional limit [10].

Even a well-studied low-temperature superconductor such as Pb has a nagging inconsis-

tency between the experimentally extracted $\alpha^2 F$ and μ^* and the bulk transition temperature T_c . The extracted dimensionless electron-phonon coupling strength λ satisfies $\lambda = 1.55$, and the Coulomb pseudopotential is $\mu^* = 0.131$ [5]. However, the Coulomb pseudopotential must be increased to $\mu^* = 0.144$ [11] in order to produce the correct T_c of 7.19K. It is possible that including the vertex corrections can explain this discrepancy.

Furthermore, new computational strategies have been developed that greatly improve the accuracy of the Migdal-Eliashberg formalism, and allow for a straightforward generalization to the incorporation of the lowest-order vertex corrections: (i) use of the local approximation for the many-body problem [12]; (ii) performing exact analytic continuations from the imaginary axis to the real axis [13]; and (iii) incorporation of high-frequency resummation schemes [14,15]. We employ all three strategies in our computational methods.

The electronic self-energy and the irreducible vertex function for superconducting order including the lowest-order vertex correction beyond the conventional model are both illustrated in Figure 1. The wavy lines denote dressed phonon propagators, and the solid lines denote dressed electronic Green functions in the Nambu-Gorkov formalism. We make the conventional approximations [11]: (i) neglect the angular dependence of the electron-phonon matrix elements and the phonon spectral functions, and evaluate them at the Fermi energy; (ii) neglect the energy dependence of the electronic density of states $\rho(\epsilon)$ and evaluate it at the Fermi energy $\rho(0)$; and (iii) treat the Coulomb interactions via a pseudopotential for the anomalous self-energy. When these approximations are invoked, one must solve a self-consistent perturbation theory in frequency-space only—the self-energy is replaced by a momentum-independent function that has been averaged over the Fermi surface. *These self-consistent equations are identical in form to the equations one would derive in the local approximation, valid in the large-dimensional limit [12,9].*

The perturbation theory is performed on the imaginary axis at the electronic Matsubara frequencies $\omega_n := \pi T(2n + 1)$. This allows for a proper treatment of the Coulomb pseudopotential, since the sharp cutoff lies on the imaginary, not the real axis [16]. If we make the conventional definitions for the quasiparticle renormalization $Z_n := Z(i\omega_n) = 1 - \text{Im}[\Sigma(i\omega_n)]/\omega_n$

and for the superconducting gap $\Delta_n := \Delta(i\omega_n) = \phi(i\omega_n)/Z(i\omega_n)$, then the self-consistent equations are:

$$Z_n = 1 + \frac{\pi T}{\omega_n} \sum_{l=-N}^N \lambda_l \frac{\omega_{n-l}}{\sqrt{\omega_{n-l}^2 + \Delta_{n-l}^2}} + \delta Z_n + \frac{\pi^3 T^2 C \rho(0)}{\omega_n} \sum_{l=-N}^N \sum_{l'=-N}^N \lambda_l \lambda_{l'} \frac{-\omega_{n-l} \omega_{n-l'} \omega_{n-l-l'} - 2\omega_{n-l} \Delta_{n-l'} \Delta_{n-l-l'} + \omega_{n-l-l'} \Delta_{n-l} \Delta_{n-l'}}{\sqrt{(\omega_{n-l}^2 + \Delta_{n-l}^2)(\omega_{n-l'}^2 + \Delta_{n-l'}^2)(\omega_{n-l-l'}^2 + \Delta_{n-l-l'}^2)}}, \quad (1)$$

$$\Delta_n Z_n = \pi T \sum_{l=-N}^N (\lambda_l - \mu^*) \frac{\Delta_{n-l}}{\sqrt{\omega_{n-l}^2 + \Delta_{n-l}^2}} + \pi^3 T^2 C \rho(0) \sum_{l=-N}^N \sum_{l'=-N}^N \lambda_l \lambda_{l'} \frac{-\Delta_{n-l} \Delta_{n-l'} \Delta_{n-l-l'} - 2\Delta_{n-l} \omega_{n-l'} \omega_{n-l-l'} + \omega_{n-l} \omega_{n-l'} \Delta_{n-l-l'}}{\sqrt{(\omega_{n-l}^2 + \Delta_{n-l}^2)(\omega_{n-l'}^2 + \Delta_{n-l'}^2)(\omega_{n-l-l'}^2 + \Delta_{n-l-l'}^2)}}, \quad (2)$$

where $\lambda_n := 2 \int_0^\infty d\Omega \alpha^2 F(\Omega) \Omega / (\Omega^2 + 4\pi^2 T^2 n^2)$ is the dimensionless electron-phonon coupling, $N = \frac{1}{2}(\frac{\omega_c}{\pi T} - 1)$ is the cutoff for the summations [the frequency cutoff is chosen to be six times the maximal frequency in $\alpha^2 F(\Omega)$, or $\omega_c = 6\omega_{max}$], δZ_n is defined below, and C is a Fermi-surface average for the vertex-correction terms. This average is defined by

$$C := \frac{1}{\rho^4(0)} \sum_q \left[\sum_k \delta(\epsilon_F - \epsilon_k) \delta(\epsilon_F - \epsilon_{q-k}) \right]^2 \quad (3)$$

with ϵ_F the Fermi energy and ϵ_k the band structure. In a free-electron model, with a k^2 dispersion, the constant C assumes the form $C = \frac{1}{6n}$, with n the number of free electrons per spin per unit cell [7]. Since the DOS at the Fermi level for a free-electron model is $\rho(0) = \frac{3n}{2\epsilon_F}$, the product $C\rho(0)$ is $\frac{1}{4\epsilon_F}$ for a free-electron model. For Pb, we perform a scalar relativistic density-functional calculation of the band structure in the local-density approximation, and find $\rho(0) = 2.5 \times 10^{-4}$ states/spin/meV, and $C = 0.15$, yielding $C\rho(0) = 4 \times 10^{-5}$ states/spin/meV. This is the value we use for the numerical work.

Finally, a high-frequency resummation scheme [14,15] is employed, that calculates the perturbation-theory results relative to the exact results for the normal state, namely

$$Z_n(\text{normal}) = 1 + \frac{1}{2n+1} [\lambda_0 + 2 \sum_{m=1}^n \lambda_m] \quad , \quad (4)$$

by appending the normal state results to the perturbation theory illustrated in Figure 1. This is achieved by adding the contribution

$$\delta Z_n := Z_n(\text{normal}) - 1 - \frac{1}{2n+1} \sum_{m=-N}^N \lambda_m \text{sgn}(n - m - \frac{1}{2}) \quad , \quad (5)$$

[where $\text{sgn}(x)$ is 1 if $x > 0$ and -1 if $x < 0$] to the perturbation series. The term δZ_n is the normal-state contribution to the quasiparticle renormalization factor that is usually neglected when one introduces the cutoff N into the frequency summations.

The difficult step in the tunneling-inversion program is to analytically continue the gap function to the real axis, in order to determine the tunneling DOS $N(\omega)$ from

$$N(\omega) = N(0) \text{Re} \left[\frac{\omega}{\sqrt{\omega^2 - \Delta^2(\omega)}} \right] \quad . \quad (6)$$

Recently, however, it was discovered that an exact analytic continuation could be performed by following the prescription of Baym and Mermin [17]: formally perform the analytic continuation $i\omega_n \rightarrow \omega + i\delta$, and then add a function that vanishes at each of the Matsubara frequencies, and is bounded in the upper half-plane except for simple poles located at just the positions necessary to cancel the poles introduced by the formal analytic continuation. Since the analytic continuation is unique, and since the final function can be shown to be analytic in the upper half-plane, this analytic-continuation procedure is exact. Such a scheme has already been implemented for the Migdal-Eliashberg theory [13], and it is a straightforward but tedious procedure to generalize these results to include the lowest-order vertex corrections. The end result is a formula for the quasiparticle renormalization, and the gap, on the real axis, that involves the data on the imaginary axis and integrals of the Green function evaluated in the upper half-plane. Because of the dependence on the Green function, these equations require a self-consistent solution on a real-axis grid (a step size of 0.05 meV is chosen for the grid spacing). The final equations are cumbersome and will be shown elsewhere.

Finally, we use this formalism to extract both $\alpha^2 F(\Omega)$ and μ^* from the experimental data. We follow the original prescription of McMillan and Rowell [5]: (i) Guess an initial value for $\alpha^2 F(\Omega)$. (ii) Adjust μ^* to reproduce the experimental superconducting gap at zero temperature Δ_0 [which is defined from $\text{Re}\Delta(\omega) = \omega$ at $\omega = \Delta_0$]. An analytic continuation

employing a Padé approximation is used to determine μ^* , since Δ_0 is determined to an accuracy of one part in 10^5 with such an approximation. (iii) Compute the functional derivative of the change in the tunneling DOS with respect to a change in $\alpha^2 F(\Omega)$. (iv) Determine the shift in $\alpha^2 F$ by solving the matrix equation

$$\int d\Omega \frac{\delta N(\omega)}{\delta \alpha^2 F(\Omega)} \delta \alpha^2 F(\Omega) = N(\omega) - N_{exp}(\omega) \quad . \quad (7)$$

This expression is discretized on the real axis, and a singular-value-decomposition is employed to determine the shift $\delta \alpha^2 F(\Omega)$, since there are small eigenvalues of the functional derivative matrix, which cause instabilities in updating $\alpha^2 F$. (v) Determine the new $\alpha^2 F(\Omega)$ by adding a smoothed shift $\delta \alpha^2 F(\Omega)$ to it, with $\alpha^2 F$ forced to behave quadratically in Ω for $\Omega < 0.5$ meV. This procedure is iterated until convergence is reached.

The results for the tunneling inversion for Pb for both the Migdal-Eliashberg theory, and the vertex-corrected theory are presented in Table 1. Various parameters are recorded including λ , the “average” phonon frequency $\omega_{ln} := \exp[2 \int_0^\infty d\Omega \ln(\Omega) \alpha^2 F(\Omega) / \Omega \lambda]$, the area A under $\alpha^2 F$, μ^* , Δ_0 , T_c , the maximum error, and the root-mean-square error of the fit. Note how a proper treatment of the cutoff for μ^* and inclusion of the high-frequency resummation improves the calculated T_c and that the vertex corrections modify λ by the order of 1% even though the Migdal parameter $[C\rho(0)\omega_{max}\lambda]$ is on the order of 0.0007. A plot of the extracted $\alpha^2 F(\Omega)$ is given in Figure 2(a). The vertex-corrected fit is the solid line and the Migdal-Eliashberg fit is the dashed line. The difference between the two spectral functions $\alpha^2 F_V(\Omega) - \alpha^2 F_{ME}(\Omega)$ is plotted in Figure 2(b). The vertex corrections produce slight enhancements to the transverse and longitudinal phonon peaks and they suppress the spectral weight in the region beyond the maximal bulk phonon frequency for Pb (about 9 meV). Finally a comparison of the fitted tunneling DOS is compared to the experimental data [5] in Figure 3. The small dots are the experimental data points used in the fitting procedure; the larger dots (from data taken at a higher temperature) were not used in the fit. The solid line is the vertex-corrected DOS and the dotted line is the Migdal-Eliashberg DOS. Note that the two curves lie on top of each other for low energy, but deviate more at

higher energies. It is difficult to tell which fit is more accurate.

We conclude with a discussion of the general properties of vertex corrections. In the conventional model, where the momentum dependence of the electron-phonon matrix elements is neglected, and the electronic DOS is assumed to be constant, the vertex corrections will always cause a reduction to T_c and the isotope coefficient α . A generalization of the formula for the Holstein model [9] shows that the ratio of the vertex-corrected T_c to the Migdal-Eliashberg T_c is

$$\frac{T_c(\text{vertex})}{T_c(\text{no vertex})} = \exp \left[-\frac{2\pi^2 C \rho(0)}{\lambda} \left(\int_0^\infty d\Omega \alpha^2 F(\Omega) + \frac{1}{\lambda} \int_0^\infty d\Omega \alpha^2 F(\Omega) \int_0^\infty d\Omega' \alpha^2 F(\Omega') \frac{1}{\Omega + \Omega'} \right) \right], \quad (8)$$

in the weak-coupling limit (if we set $\mu^* = 0$). This formula gives an order-of-magnitude estimate for when effects of vertex corrections should be important in a real material (for Pb the ratio is 0.9978).

The other main effect of vertex corrections is that they will modify the higher-energy structure in $\alpha^2 F(\Omega)$, because they involve processes where two phonons scatter, so that the structures in $\alpha^2 F(\Omega)$ are changed at multiples of the lower-energy peaks. This effect is small in a low-temperature superconductor, but could be significant in the newly discovered superconductors.

Finally, the vertex corrections will also modify the isotope coefficient. It is possible that effects of vertex corrections could be seen upon reexamination of isotope coefficient data on low-temperature superconductors. Work in this direction is currently in progress. We also plan on extracting $\alpha^2 F$ and μ^* for other low-temperature superconductors to see if the effects of vertex corrections are important in other materials. We plan on applying the vertex-corrected tunneling inversion program to both $\text{Ba}_{1-x}\text{K}_x\text{BiO}_3$ and the doped fullerenes once accurate tunneling data for these materials becomes available.

We would like to acknowledge useful discussions with J. Carbotte, D. Hess, M. Jarrell, V. Kostur, F. Marsiglio, B. Mitrović, J. Rowell, D. Scalapino, H.-B. Schüttler, and J. Serene. J. K. F. acknowledges the Donors of The Petroleum Research Fund, administered

by the American Chemical Society (ACS-PRF No. 29623-GB6) and the Office of Naval Research Young Investigator Program (N000149610828) for partial support of this research. E. J. N acknowledges support from the Natural Sciences and Engineering Research Council of Canada (NSERC).

REFERENCES

- [1] A. B. Migdal, Zh. Eksp. Teor. Fiz. **34**, 1438 (1958) [Sov. Phys.–JETP **7**, 999 (1958)].
- [2] G. M. Eliashberg, Zh. Eksp. Teor. Fiz. **38**, 966 (1960) [Sov. Phys.–JETP **11**, 696 (1960)].
- [3] L. F. Mattheiss, E. M. Gyorgy, and D. W. Johnson, Jr., Phys. Rev. B **37**, 3745 (1988); R. J. Cava, et al., Nature **322**, 814 (1988).
- [4] A.F. Hebard, et al., Nature **350**, 600 (1991); K. Holczer, et al., Science **252**, 1154 (1991); M.J. Rosseinsky, et al., Phys. Rev. Lett. **66**, 2830 (1991).
- [5] W. L. McMillan and J. M. Rowell, Phys. Rev. Lett. **14**, 108 (1965); in *Superconductivity*, edited by R. Parks (Marcel Dekker, Inc., New York, 1969), Vol. 1, p. 117.
- [6] M. Grabowski and L. J. Sham, Phys. Rev. B **29**, 6132 (1984).
- [7] V. N. Kostur and B. Mitrović, Phys. Rev. B **48**, 16388 (1993); Phys. Rev. B **50**, 12774 (1994).
- [8] L. Pietronero, S. Strassler, C. Grimaldi, Phys. Rev. B **52**, 10516 (1995); C. Grimaldi, L. Pietronero, S. Strassler, Phys. Rev. B **52**, 10530 (1995); Phys. Rev. Lett. **75**, 1158 (1995).
- [9] J. K. Freericks and D. J. Scalapino, Phys. Rev. B **49**, 6368 (1994); J. K. Freericks, Phys. Rev. B **50**, 403 (1994); J. K. Freericks and Mark Jarrell, Phys. Rev. B **50**, 6939 (1994); E. J. Nicol and J. K. Freericks, Physica C **235–240**, 2379 (1994).
- [10] J. K. Freericks, M. Jarrell, and D. J. Scalapino, Phys. Rev. B **48**, 6302 (1993); Europhys. Lett. **25**, 37 (1994); J. K. Freericks and M. Jarrell, Phys. Rev. Lett. **75**, 2570 (1995).
- [11] *Superconductivity*, edited by R. Parks (Marcel Dekker, Inc., New York, 1969); P. B. Allen and B. Mitrović, Solid State Phys. **37**, 1 (1982); J. P. Carbotte, Rev. Mod. Phys. **62**, 1027 (1990).
- [12] W. Metzner and D. Vollhardt, Phys. Rev. Lett. **62**, 324 (1989).

- [13] F. Marsiglio, M. Schossmann, and J. P. Carbotte, *Phys. Rev. B* **37**, 4965 (1988).
- [14] F. Marsiglio, unpublished.
- [15] J.J. Deisz, D.W. Hess, and J.W. Serene, *Recent Progress in Many-Body Theories*, vol. 4, edited by E. Schachinger, et al., 433 (Plenum, New York, 1995).
- [16] C. R. Leavens and E. W. Fenton, *Solid State Commun.* **33**, 597 (1980).
- [17] G. Baym and N. D. Mermin, *J. Math. Phys.* **2**, 232 (1961).

TABLES

TABLE I. Comparison of fitted tunneling inversion data for the Migdal-Eliashberg theory and the vertex-corrected theory. The vertex corrections modify λ by the order of 1%.

Theory	λ	ω_{ln} (meV)	A (meV)	μ^*	Δ_0 (meV)	$T_c(K)$	max. error	r.m.s. error
Migdal-Eliashberg	1.542	4.863	4.029	0.136	1.400	7.23	0.0004	0.0001
Vertex-Corrected	1.561	4.847	4.070	0.141	1.400	7.22	0.0007	0.0001

FIGURES

(a)

$$-i\Sigma = \text{[diagram 1]} + \text{[diagram 2]}$$

(b)

$$\text{[diagram 1]} + \text{[diagram 2]} + \text{[diagram 3]} + \text{[diagram 4]}$$

FIG. 1. Feynman diagrams for (a) the electronic self-energy and (b) the irreducible vertex function in the superconducting channel. The first diagram in (a) and (b) is the Migdal-Eliashberg approximation, the remaining diagrams are the lowest-order vertex corrections. The solid lines denote dressed electron propagators and the wiggly lines denote dressed phonon propagators.

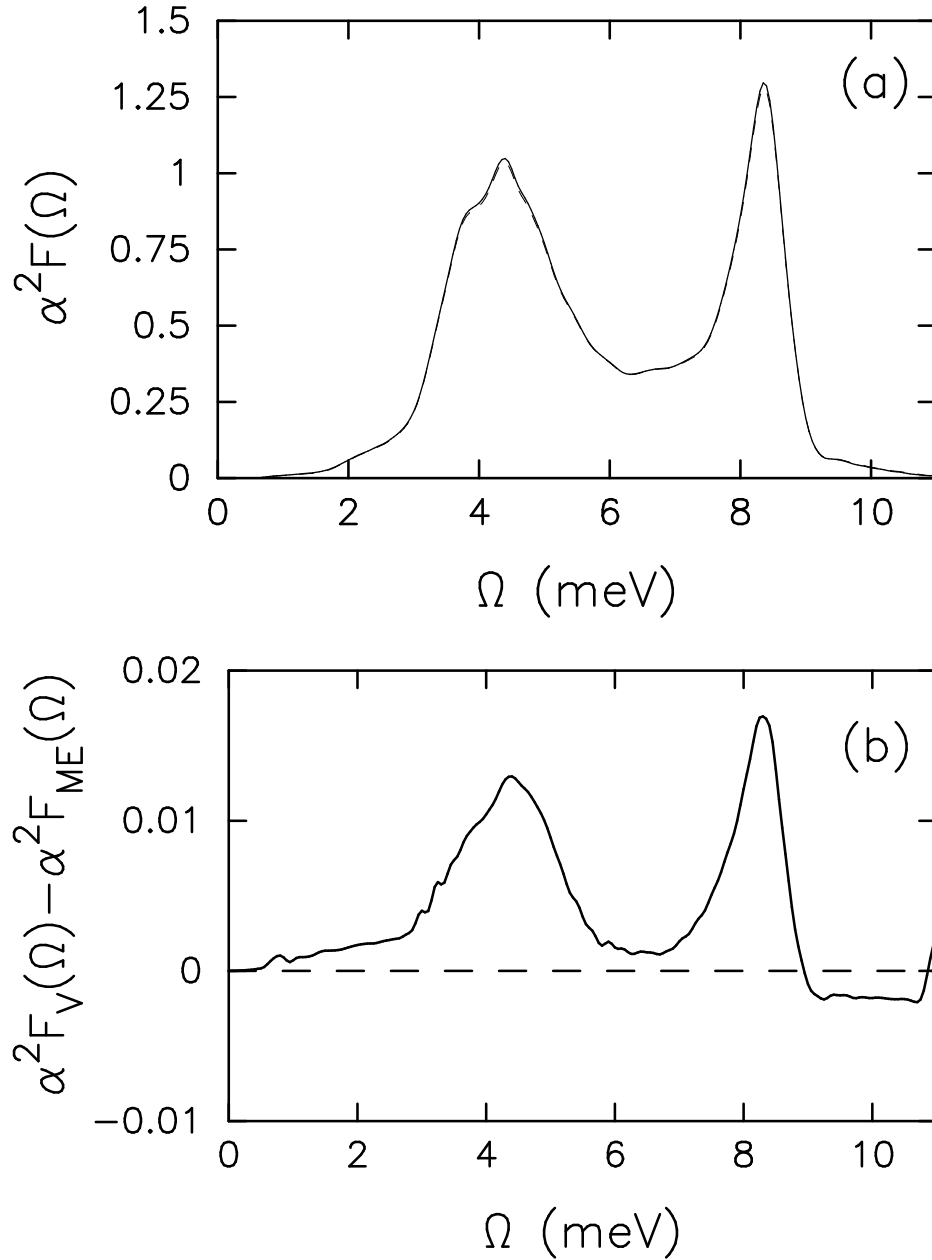


FIG. 2. (a) Electron-phonon spectral function, $\alpha^2 F(\Omega)$, extracted from the experimental tunneling data for Pb. The solid line is the vertex-corrected fit and the dashed line is the Migdal-Eliashberg fit. (b) Difference in extracted spectral functions $\alpha^2 F_V(\Omega) - \alpha^2 F_{ME}(\Omega)$. Note the enhancement of the peaks and the suppression in the region where Ω is larger than the maximum phonon frequency in bulk Pb.

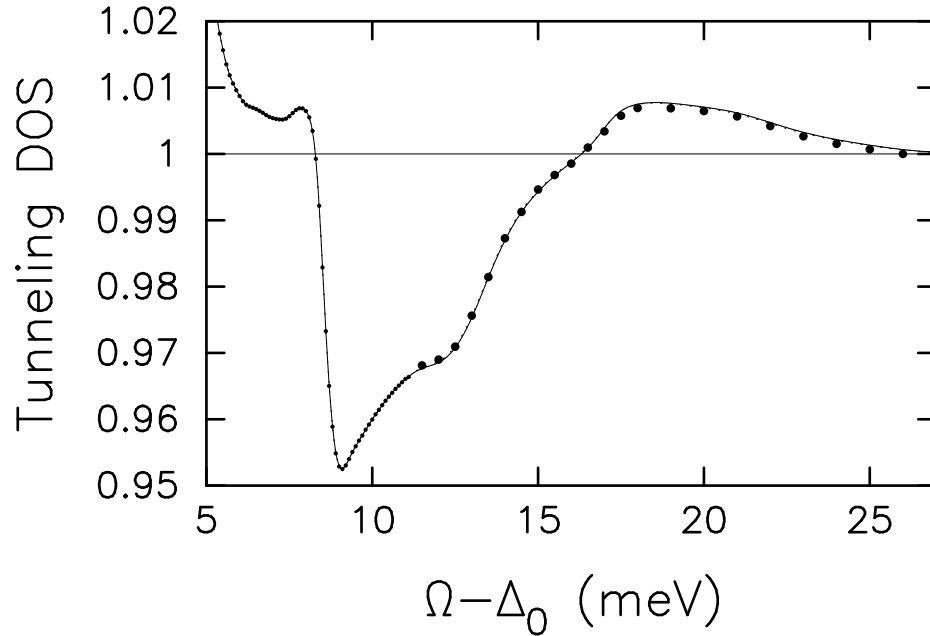


FIG. 3. Comparison of the experimental tunneling DOS (solid dots) to the fitted DOS for Pb. The solid line is the vertex-corrected fit and the dotted line is the Migdal-Eliashberg fit. The small dots are the experimental data included in the fit, while the large dots are experimental data not included in the fit, but taken at a higher temperature (and hence less accurate).